

# INVESTIGATING THE INTERSTELLAR MEDIUM STRUCTURE AND POROSITY TO IONIZING PHOTONS IN LOCAL PRIMITIVE GALAXIES

L. Ramambason<sup>1</sup> and V. Lebouteiller<sup>1</sup>

**Abstract.** Part of the ionizing continuum (Lyman continuum, LyC) produced by young stars can leak out of the host galaxy and ionize its surroundings. At high redshift, such LyC-leaking galaxies are among the best candidates to fully account for reionization (Robertson et al. 2013). However, direct measurements are extremely difficult as the LyC photons are easily absorbed by neutral gas on the observed line of sight. Instead, indirect tracers have been used to probe the structure of the interstellar medium (ISM) (e.g. Lyman alpha line, absorption lines) but such methods are also sensitive to line of sight selection effects. Using integrated emission lines in the optical and infrared domain mostly palliates viewing angle dependencies; it is a promising method to make the most of observations with current ground-based facilities (e.g., ALMA) and upcoming space missions (e.g., JWST) that will grant access to many spectroscopic tracers up to redshift above 7. However, a complex modeling step is much needed to take into account the available tracers originating in different phases and to consider a multi-component topology which matches the ISM signatures of known leaking galaxies (Ramambason et al. 2020). Such complex representative models are crucial to investigate morphology-dependent questions such as the impact of the metal and dust content on the gas distribution and mass in the different reservoirs and the porosity to ionizing radiation. Local low-metallicity galaxies, with quasi-primordial-like physical conditions and with numerous emission lines available, are ideal laboratories to benchmark this new method and explore its predictive power in high-redshift galaxies for which only a few tracers are often observed. To constrain the parameters of this representative galaxy model, we co-developed MULTIGRIS (Lebouteiller & Ramambason in prep.) a new Bayesian code using MCMC sampling. Among the various applications, MULTIGRIS can produce probability density functions of physical parameters, either primary (density, ionization parameter, stellar population age etc...) or secondary (ionizing photon escape fraction, dust mass, H2 mass etc...). I present here the first results obtained on the Dwarf Galaxy Survey (Madden et al. 2013), a sample of local, low-metallicity galaxies using combinations of Cloudy models (Ferland et al. 2017). We build upon previous results from Cormier et al. (2019) to quantify the larger porosity of the interstellar medium for low-metallicity galaxies, with the inferred topology having more density bounded regions, leading to photons escaping the HII regions. We explore dependencies of ionizing photons escape fraction on our model parameters and discuss promising line ratios for future local- and high-redshift studies.

Keywords: interstellar medium, emission lines, primitive galaxies, escape fraction

## 1 Introduction

Current observations available in the local and high-redshift universe are limited by spatial resolution and detection limit. Detailed studies of the ISM are especially challenging due the blending of emission arising from the different phases (e.g. H II regions, neutral atomic hydrogen and neutral molecular gas) into one single beam sight and potential multi-modal density distributions within a single ionization phase. To disentangle the contribution of each phase, we propose to use a representative topology which combines different sectors having different physical parameters. This approach is an intermediate step between simplistic geometries of classical photo-ionization/photo-dissociation code such as Cloudy (Ferland et al. 2017) and 3D radiative transfer codes and simulations which account for very complex gas distribution but have degrees of freedom that can hardly be constrained by observations. Our "topological" model introduces a layer of complexity which provide a more realistic picture of the multiphase ISM while keeping a relatively modest number of free parameters that

---

<sup>1</sup> AIM, CEA, CNRS, Université Paris-Saclay, Université Paris Diderot, Université de Paris, F-91191, Gif-sur-Yvette, France.

can be constrained with a only few emission lines. Similar approaches have successfully been used in previous studies (see Section 2) where the free parameters of models were tuned to match observation using frequentist methods (i.e.,  $\chi^2$ ). We build on those results to develop a more general tool that will provide a new Bayesian framework to study the multiphase ISM and specifically some quantities of interest such as the LyC photons escape fraction.

## 2 Topological models

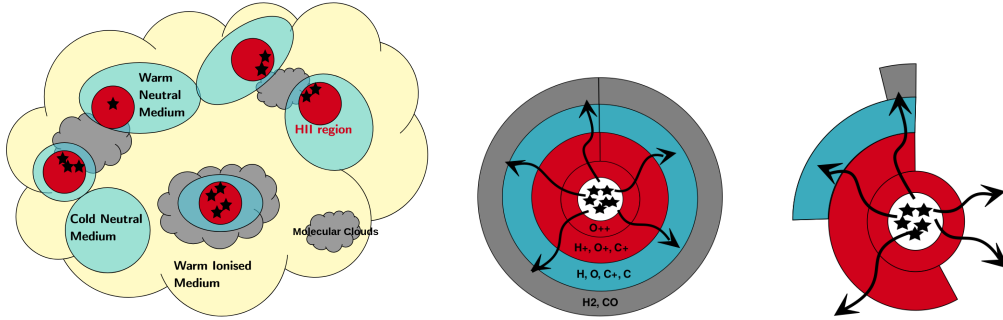


**Fig. 1.** **Left:** Schematic view of the main phases of the ISM. **Right:** Two possible representative topologies (1 sector and 4 sectors).

Topological models are refined multi-sector and multi-phase models representing the contribution of each phase (see Figure. 1) to the total emission. They were first introduced in Péquignot (2008) on a test case study on the proto-typical, low-metallicity galaxy IZw18. Figure 1 shows a schematic view of the multiphase ISM and two representative topologies with either one sector or 4 sectors stopping at different depths. Such models have been refined and successfully applied to local objects (e.g. Haro11: Cormier et al. 2012, IZw18: Leboutteiller et al. 2017, IC10: Polles et al. 2019), to sample of galaxies (e.g., DGS: Cormier et al. 2019) and resolved regions in the SMC/LMC (Lambert-Huygues et al. in prep.). The results from those studies indicate that the inclusion of density-bounded regions and non-unity PDR covering factor are necessary to reproduce the emission lines of most local objects. Such findings are at odds with UV observations which detect little to no LyC in the local universe. (e.g., Bergvall et al. 2006; Leitet et al. 2013; Borthakur et al. 2014; Leitherer et al. 2016). Results from Polles et al. (2019) indicate that the observed spatial scale drives the estimated porosity of the regions, with most clouds being matter-bounded at small scales while regions become more and more radiation-bounded at galactic scale. Using the best fitting model between 1-sector and 2-sectors configurations, Cormier et al. (2019) shows that the PDR covering factor varies with metallicity, lower metallicity leading to lower PDR covering factors. This might be suggestive of an increased porosity of the ISM at lower metallicity that might favor LyC photons escape. However a quantitative estimate of the amount photons leaking out of H II regions is yet to be determined as well as the physical mechanisms describing the variation of the escape fraction.

## 3 MULTIGRIS: a new Bayesian framework for ISM studies

MULTIGRIS (Leboutteiller & Ramambason in prep.) is a new Bayesian code designed to use emission lines to constrain the probability density functions (PDF) of various parameters from our topological models.

### 3.1 Grids of photo-ionization models

We use the photo-ionization and photo-dissociation code Cloudy c17.02 (Ferland et al. 2017) to create the models that will be combined as sectors around a representative cluster. Each model consists in a spherical shell of gas placed at a fixed inner radius of the incident radiation source within a single sector. We use a closed, spherical geometry which take into account the transmitted and reflected radiation. Radiative transfers are computed along each line of sight (1D) in a continuous way throughout the H II region, PDR and molecular zone. A detailed description of the grid will be presented in Ramambason et al. (in prep.). The models are then combined to create a representative topology in which the emission lines are computed as weighted linear

combination of the emission line from each sector. Other physical quantities available in Cloudy can also be combined as long as they scale with luminosity and can be combined as linear function of sectors (e.g., gas masses in the different phases, number of ionizing photons  $Q_{\text{ion}}$ ...). We calculate the global escape fraction of photons for a given topology by using the ionizing continuum provided by Cloudy at each depth in the model.

### 3.2 Bayesian framework

MULTIGRIS can be used with different Monte Carlo samplers which will be described in the benchmark paper (Lebouteiller & Ramambason in prep.). For this study we run MULTIGRIS at order 0 which performs a nearest neighbour interpolation in the grid of Cloudy models. In the following example we used the SMC sampler from PyMC3 (Salvatier et al. 2016). We define the likelihood of our data  $P(d|\theta)$  by considering our suite of emission lines as independent identically distributed random variable (RV). Each RV can be chosen to follow either an asymmetric gaussian law centered on the measured value or an asymmetric StudentT law. In this study we consider use a Student-T distribution for each RV with a normality parameter  $\nu=1$ . Hence the likelihood is given by:

$$\mathcal{L} = P(d|\theta) = \prod_{i=0}^N \mathcal{S}(\nu = 1, \mu = O_i, \sigma^2 = U_i^2), \quad (3.1)$$

where  $\nu$  is the normality parameter of the Student-T distribution,  $N$  the number of emission lines with observed fluxes  $O_i$  and uncertainties  $U_i$ . For undetected lines with instrumental upper limit, the Student-T distribution is replaced by a half-Student-T likelihood with the same normality parameter  $\nu$ . For lower and upper limits, the  $\sigma$  corresponds to the RMS of the signal and reflects the uncertainty on the limit itself.

### 3.3 Example of application on the Dwarf Galaxy Survey

On Figure 2, we show an example of the application of MULTIGRIS to the galaxy IZw18. For each galaxy, several configurations can be tested (i.e., with different number of sectors, different prior on the luminosity, metallicity etc...).

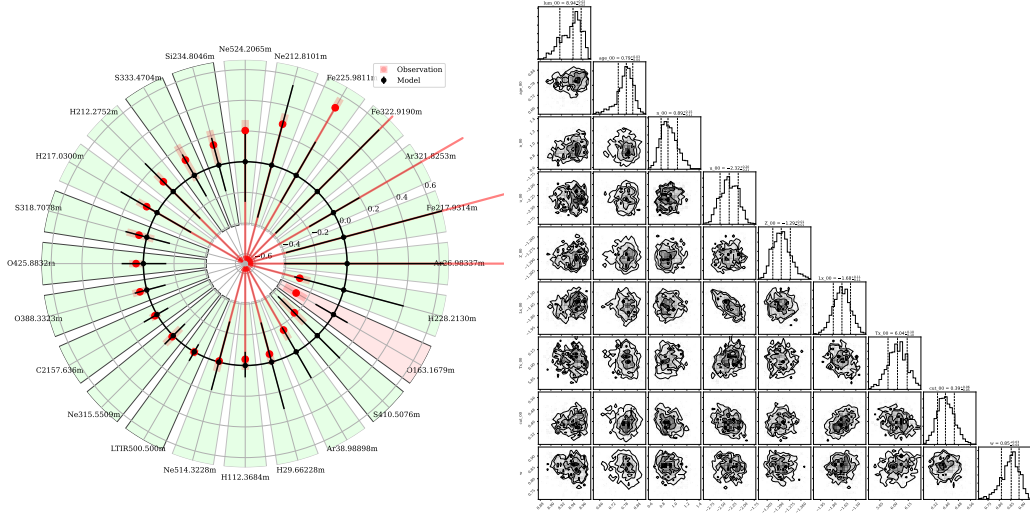


**Fig. 2.** Some diagnostic plots for galaxy IZw18, for a 3-sectors configuration. **Left:** Plot showing the agreement of predicted line fluxes with measured lines. Arrows represent instrumental upper limits. **Right:** Corner plot showing the PDF of primary parameter for one of the 3 sectors.

We applied MULTIGRIS to a sample of 38 compact, fully observed galaxies with at least three spectral lines detected among the 50 galaxies observed in the Herschel Dwarf Galaxy Survey (Madden et al. 2013). On Figure 3, we show the best models for each galaxy selected based on the Leave-One-Out cross validation (LOO) criterium (Vehtari et al. 2017) among 6 configurations having different number of sectors (1,2 or 3) and different

model luminosity\* ( $L=10^7 L_{\odot}$  or  $10^9 L_{\odot}$ ). Our results confirm the trend from Cormier et al. (2019) of increasing porosity of the ISM at low metallicity. We note that there seems to be a bimodality in our sample, with two branches of leaking and non-leaking galaxies clearly visible on the Kernel Density Estimate (KDE). The globally high escape fractions we find correspond to the fractions in the hypothesis that H II regions dominate the integrated spectrum of the galaxy, with in particular the diffuse ionized gas component and the neutral gas envelope being ignored for now. Those limits as well as other dependencies of the escape fraction will be further discussed in Ramambason et al. (in prep.).

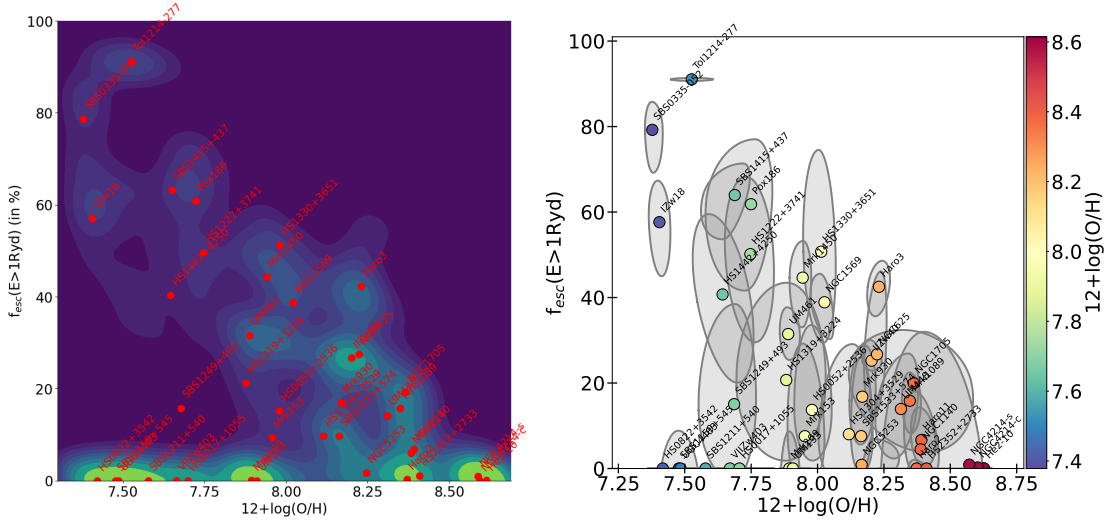


**Fig. 3.** Evolution of the inferred escape fraction from H II regions with respect to the inferred metallicity. **Left:** KDE representation, the red dots represent median values for each galaxy. **Right:** Skewed uncertainty ellipsis (SUE, Galliano et al. 2021) A SUE represents the  $1\sigma$  contour of a 2 dimensional split-normal distribution adjusted to have the same three first moment as the underlying PDF.

## References

- Bergvall, N., Zackrisson, E., Andersson, B. G., et al. 2006, *A&A*, 448, 513  
 Borthakur, S., Heckman, T. M., Leitherer, C., & Overzier, R. A. 2014, *Science*, 346, 216  
 Cormier, D., Abel, N. P., Hony, S., et al. 2019, *A&A*, 626, A23  
 Cormier, D., Lebouteiller, V., Madden, S. C., et al. 2012, *A&A*, 548, A20  
 Ferland, G. J., Chatzikos, M., Guzmán, F., et al. 2017, *Rev. Mexicana Astron. Astrofis.*, 53, 385  
 Galliano, F., Nersesian, A., Bianchi, S., et al. 2021, *A&A*, 649, A18  
 Lambert-Huygues et al., A. in prep.  
 Lebouteiller, V., Péquignot, D., Cormier, D., et al. 2017, *A&A*, 602, A45  
 Lebouteiller, V. & Ramambason, L. in prep.  
 Leitet, E., Bergvall, N., Hayes, M., Linné, S., & Zackrisson, E. 2013, *A&A*, 553, A106  
 Leitherer, C., Hernandez, S., Lee, J. C., & Oey, M. S. 2016, *ApJ*, 823, 64  
 Madden, S. C., Rémy-Ruyer, A., Galametz, M., et al. 2013, *PASP*, 125, 600  
 Péquignot, D. 2008, *A&A*, 478, 371  
 Polles, F. L., Madden, S. C., Lebouteiller, V., et al. 2019, *A&A*, 622, A119  
 Ramambason, L., Schaerer, D., Stasińska, G., et al. 2020, *A&A*, 644, A21  
 Ramambason et al., L. in prep.  
 Robertson, B. E., Furlanetto, S. R., Schneider, E., et al. 2013, *ApJ*, 768, 71  
 Salvatier, J., Wiecki, T. V., & Fonnesbeck, C. 2016, *PeerJ Computer Science*, 2, e55  
 Vehtari, A., Gelman, A., & Gabry, J. 2017, *Stat Comput* 27, 1413–1432

\*The model luminosity is scaled with a free parameter to match the observed luminosity of each galaxy. Different model luminosities result in different geometry of the models.